GAS-LIQUID INTERFACIAL AREA AND LIQUID-PHASE MASS TRANSFER COEFFICIENT IN SIEVE PLATE COLUMNS WITHOUT DOWNCOMER OPERATING AT HIGH GAS VELOCITIES

TOSHIRO MIYAHARA, MASAKI KURIHARA, MITSUHIRO ASODA AND TERUO TAKAHASHI

Department of Applied Chemistry, Okayama University, Okayama 700

Key Words: Sieve Plate Column, Interfacial Area, Mass Transfer Coefficient, High Gas Velocity, Large Free Area

Experiments were performed to investigate the gas-liquid interfacial area and the liquid-phase mass transfer coefficient of a two-phase dispersion on sieve plates with hole diameters of 4–12 mm and with free areas of 5.5–50.4% without downcomer. Operation was carried out at high gas velocities using cobalt-catalyzed oxidation of aqueous sodium sulfite solution with air.

The two-phase dispersion showed froth regime and transition regime, which is called partially developed spray regimes/mixed froth regimes, depending on the gas velocities. The gas-liquid interfacial area of the two-phase dispersion in the froth regime is influenced by the free area of the plate, whereas no effect of free area is found in the transition regime. The correlations of interfacial area for each regime are given on the basis of the correlation obtained by Zuiderweg under a gas-liquid cross-current condition. Empirical equations for the Sherwood number based on liquid depth are obtained. Using the results of the interfacial area and the mass transfer coefficient, the mass transfer volumetric coefficient can be predicted.

Introduction

The plate column without downcomer is widely used in a range of applications such as distillation and/or absorption because of its inexpensive and simple construction. Recently, in the interests of energy conservation, high-capacity gas-liquid contacting devices applicable to operation at high gas velocities have come into demand. Low pressure drop, leading to the use of sieve plates with large free areas, should be a necessary condition for the operation of these devices. Kimura *et al.*[5] studied experimentally the stable operating ranges and gas-liquid holdups for sieve plates without downcomers and having large free areas. The authors[20] have also investigated pressure drop, liquid holdup and operating ranges for plates having large free areas. However, data available for the design of devices for mass transfer characteristics are only for plates with small free areas and with small hole diameters. Further, as mentioned in the review by Zuiderweg,[23] almost all the data are for plates under gas-liquid cross-current flow conditions, and the applicability for the results for plates with small free areas to those with large free areas must be open to doubt.

In the present study, experiments were performed with plates without downcomer having a large free area and capable of being operated at high gas velocities. Gas-liquid interfacial area, liquid-phase mass transfer and volumetric mass transfer coefficients of the sieve plate column were studied with a cobalt-catalyzed oxidation of aqueous sodium sulfite solutions by air.

Received July 24, 1989. Correspondence concerning this article should be addressed to T. Miyahara.

1. Experimental

1.1 Experimental apparatus and procedure

The experimental apparatus is schematically shown in **Fig. 1**. A 10.4-cm-diameter Plexiglas column fitted with three plates at a plate spacing of 60 cm was used.

Sieve plates were made of 1 mm-thick aluminium sheet with hole diameters between 4–12 mm arranged in equilateral triangles corresponding to free areas of 5.5–50.4% respectively. Details are shown in **Table 1**.

Aqueous sodium sulfite solutions from the tank passed through the head tank and were supplied to the top plate from the circumference through the liquid distributor installed in the column top after the orifice measured the flow of liquid. The solution then made contact with the gas on each plate and was discharged from the column base. Plates of polystyrene foam were placed on the liquid surface in both the storage tank and the head tank to minimize the oxidation of sodium sulfite. The amount of liquid on each plate was measured by a calibrated level guage connected to the column wall.[11] Liquid temperatures were measured with thermometers. After measuring the air flow rate

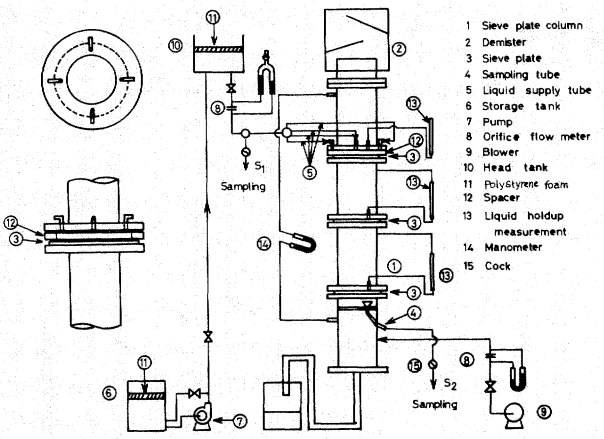


Fig. 1. Experimental apparatus

Table 1. Geometries of sieve plates

Plate	Hole dia. $d\times10^3$ [m]	Pitch $p\times10^3$ [m]	F [—]	$U_L\times10^2$ [m/s]	Key
P-1	4.0	15.0	0.055	0.05–0.15	○
P-2	4.0	12.0	0.081	0.05–0.15	●
P-3	4.0	11.0	0.107	0.051–0.236	△
P-4	4.0	7.6	0.241	0.051–0.236	■
P-5	4.0	5.5	0.463	0.1–0.389	▽
P-6	6.0	8.0	0.463	0.1–0.389	◩
P-7	8.0	11.0	0.504	0.1–0.389	◪
P-8	12.0	16.0	0.493	0.1–0.389	□

from the blower the air entered the column base, dispersed into the liquid through the sieve plate and was vented from the column top after gas-liquid separation by the demister.

After 20–25 minutes from steady state, liquid samples were taken at the feed pipe (S_1) as inlet liquid and at the glass funnel installed 3 cm beneath the base plate as outlet liquid. The samples were analyzed for sodium sulfite content by iodometric back-titraction. Concentrations of sodium sulfite fed into and discharged from the column were obtained. Concentrations of cobaltous sulfate used for this test as the oxidation catalyst were determined by atomic absorption analysis. When foreign cupric ions are present in the solution, the reaction will be enhanced. Thus materials such as copper, bronze and brass were not used.

We used polyvinyl chloride tubes for the liquid supply, and valves in contact with the liquid were made of stainless steel or polyvinyl chloride. For the same reason, sieve plates for this test were made of aluminum sheet.

1.2. Measurement of gas-liquid interfacial area and liquid-phase volumetric mass transfer coefficient

Oxidation of aqueous sodium sulfite solution with oxygen using cobalt sulfate as a catalyst, which is a liquid film-controlled instantaneous pseudo-second order reaction, can be expressed as follows:

$$2Na_2SO_3+O_2\xrightarrow{Co^{++}}2Na_2SO_4 \tag{1}$$

The sulfite oxidation has been determined to be first-order dependent on cobalt concentration and second-order dependent on oxygen below a partial pressure of 10^5 Pa when $C_{BL}>0.5$ mol/l and pH$\simeq$ 8.5.[6] Presuming a quite large amount of sodium sulfite compared to that of oxygen and a very large film thickness relative to the depth of penetration of solute, this reaction can be represented mathematically as

$$D_A\frac{d^2C_{AL}}{dx^2}-k_2C_{AL}^2=0 \tag{2}$$

The solution of this expression with the boundary condition $C_{AL}=0$ at $x=\infty$ and $C_{AL}=C_{Ai}$ at $x=0$ gives the following mass transfer rate.[3]

$$R_A=a_LC_{Ai}\sqrt{(2/3)k_2C_{Ai}D_A} \tag{3}$$

where $\gamma>3$, $\gamma\leqq(1/2)\beta_\infty$, $\beta_\infty=1+D_BC_{BL}/(2D_AC_A)$ and $\gamma=\sqrt{(2/3)k_2C_{Ai}D_A}/k_L$. The following equation is applicable to finding the gas-liquid interfacial area, presuming perfect mixing in the two-phase dispersion on a plate.

$$a_L=\frac{U_L(C_{B1}-C_{B2})}{2nh_LC_{Ai}\sqrt{(2/3)k_2C_{Ai}D_A}} \tag{4}$$

where a_L is the interfacial area per unit volume of liquid, and n is the number of plates. We used the following equations reported by Miller[7] for the rate constant k_2 and oxygen concentration at the interface C_{Ai}:

$$k_2=(0.263-0.15\times10^{-3}C_{BL})\times10^5C_{CoSo_4}\times\left[\frac{\mathrm{pH}-7.9+0.04t}{0.6+0.04t}\right]^2\exp\left[-8450\left(\frac{1}{T}-\frac{1}{293}\right)\right] \tag{5}$$

$$C_{Ai}=P_{O_2}/(HRT) \tag{6}$$

where

$$H=\exp(12.907-2832/T-9.665\times10^{-3}C_{BL}+3.181C_{BL}/T) \tag{7}$$

The molecular diffusivity for oxygen in sulfite solutions was calculated from

$$D_A=0.795\times10^{-14}T/\mu_L \tag{8}$$[7]

Under conditions of physical absorption obtained by decreasing the amount of cobalt sulfate, the liquid-phase volumetric mass transfer coefficient could be calculated from the equation

$$k_L a_L = \frac{U_L(C_{B1} - C_{B2})}{2nh_L C_{Ai}} \tag{9}$$

Table 2 shows the experimental conditions in the present study. The liquid-phase mass transfer coefficient can be calculated from the liquid-phase volumetric mass transfer coefficient and the interfacial area.

2. Results and Discussion

2.1 Flow regimes of the two-phase dispersion

Figure 2 shows typical photographs of the two-phase dispersion on a plate. From the photographs, the operating range can be classified into two regimes: froth regime (liquid continuous), which exists at relatively low gas flow rates, and transition regime, which may be called partially developed spray regime/mixed forth regime (partially gas continuous) close to spray regime which appears at relatively high gas velocities. Here, the transition from the fully developed forth regime to the fully developed spray regime occurs gradually and the liquid is dispersed into many droplets by the action of gas jets issuing from the plate holes. The authors *et al.*[8-9] have previously noticed transient jetting between bubbling and jetting at a single hole and between froth and spray at multiple holes from quantifying the phenomena of the transition from froth to spray on a sieve plate. The transition regime observed in the present study seems to correspond to transient jetting; Asano *et al.*[1] have also confirmed the existence of this regime. Note that the complete spray regime does not appear in plate columns without down comer because the simultaneous passage of gas and liquid through plate holes promotes bubbling and suppressed jetting at the hole.

2.2 Gas-liquid interfacial area

Many droplets scatter violently from two-phase dispersion because the operation of sieve plates having a large free area is carried out at high gas velocities, leading to a small holdup. Although gas-liquid interfacial areas have been reported on a unit froth volume basis, that is, as a_F, interfacial area based on unit volume of liquid, a_L, was considered in the present study due to the difficulty of specifying the two-phase dispersion height.

From the previous results,[18-19] gas holdup, one of the hydrodynamic characteristics of two-phase dispersion on a plate, was correlated with the Froude number based on liquid holdup, Fr. Therefore, the behavior of interfacial area, a_L, against Fr was investigated. **Figure 3** shows the values of the interfacial area for plates of P-1–P-8 together with the previous results. It is seen that the interfacial areas for plates of P-1–P-3 representing the forth regime in the present study are close to the results of

Table 2. Experimental condition

	Irreversible pseudo-second order reaction	Physical absorption
Na_2SO_3	>0.5 mol/l	>0.5 mol/l
$CoSO_4$	2×10^{-3} mol/l	$<8.5\times10^{-6}$ mol/l
pH	8.5	8.5

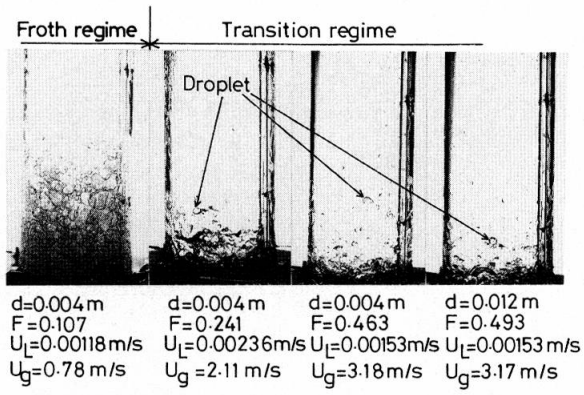


Fig. 2. Photograph of flow pattern of two-phase dispersion on a sieve plate

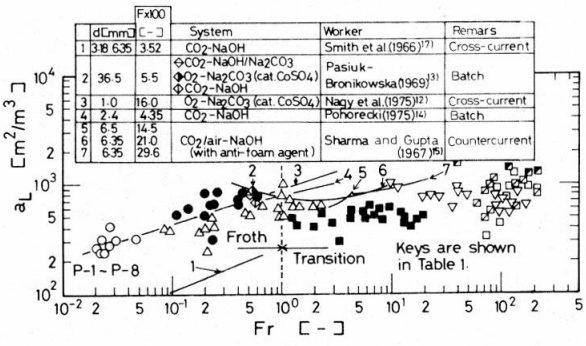


Fig. 3. Gas-liquid interfacial area

Pasiuk-Bronikowska[13] and Pohorecki[14] for batch operation and those of Nagy *et al.*[12] for gas-liquid cross-current flow, and are a little smaller than those of Sharma *et al.*[15] for plate columns without downcomer. As seen in the figure, the interfacial area in the froth regime increases as the Froude number increases, whereas no significant effect of the Froude number on the interfacial area is noticed in the transition regime. The critical Froude number is about unity, which roughly agrees with the critical value obtained by the authors.[19] The scatter of experimental values in the figure is probably explained by the liquid velocity, of which the interfacial area is a function.

Zuiderweg,[23] who made studies of gas-liquid interfacial areas under gas-liquid cross-current flow conditions in a 1.2-m plate column with sieve plates having free area of 8 and 14%, proposed the following correlations as a function of the Weber number.

$$a_w = (40/F^{0.3})We^{0.37} \quad \text{spray regime} \tag{10}$$

$$a_w = (43/F^{0.3})We^{0.53} \quad \text{mixed/emulsion flow regime} \tag{11}$$

where $a_w = a_L h_L$ and $We = h_L U_g \rho_g^{0.5} U_L \rho_L^{0.5}/\sigma$. Hence, gas-liquid interfacial areas on the basis of unit bubbling area are plotted against the Froude number in **Fig. 4** in order to examine the dependence on the hydrodynamic behavior. The values of interfacial areas are divided broadly into two regimes: froth regime (a_w > about 20 m^2/m^2) and transition regime (a_w = 5–20 m^2/m^2). Each solid line and the measurements correspond to the previous results shown in Fig. 3.

Thomas *et al.*[21-22] noticed the effect of liquid velocity on the interfacial areas under gas-liquid cross-current flow conditions, whereas Nagy *et al.*[12] and Smith *et al.*[17] denied this trend, as did Sharma *et al.*[15] for plate columns without downcomer. Although we could not find any remarkable effect of liquid velocity on the interfacial areas, the interfacial areas are larger with greater flow rate of liquid, and no significant effects due to hole diameter were found. **Figure 5** shows the correlation of the interfacial area based on unit bubbling areas as a function of the Weber number proposed by Zuiderweg.[23] As seen from the figure, the effect of the free area can be found in the forth regime, but not in the transition regime. The data for the two regimes can be correlated by

$$a_w = 80We^{0.5}/F^{0.5} \quad \text{froth regime} \tag{12}$$

$$a_w = 19.1We^{0.2} \quad \text{transition regime (partially developed spray/mixed froth)} \tag{13}$$

The effect of free area in the froth regime is probably explained by the fact that discrete bubbles are formed at the holes, whereas in the transition regime many droplets appear by the action of the gas jets.

2.3 Liquid-phase mass transfer coefficient

Figure 6 shows the liquid-phase mass transfer coefficient as a function of gas velocity. The values of mass transfer coefficient for plates having large free areas (P-4–P-8) are larger than those of Sharma *et al.*[14] (without downcomer), but roughly agree with those of Pohorecki[14] and Pasiuk-Bronikowaka[13] (batch operation) and those of Sharma *et al.*[16] (bubble cap).

Kawagoe *et al.*[4] studied the influence of flow patterns on the liquid-phase mass transfer coefficient and bubble size using sieve plates with downcomer having free areas of 0.621–5.59%. From the results, they reported that the variation of bubble size and mass transfer coefficient with gas velocity and liquid holdup correspond to the flow patterns; that is, bubble flow, froth and cellular foam and the values of mass transfer coefficient are maintained constant in each flow regime. The solid lines are for the results of

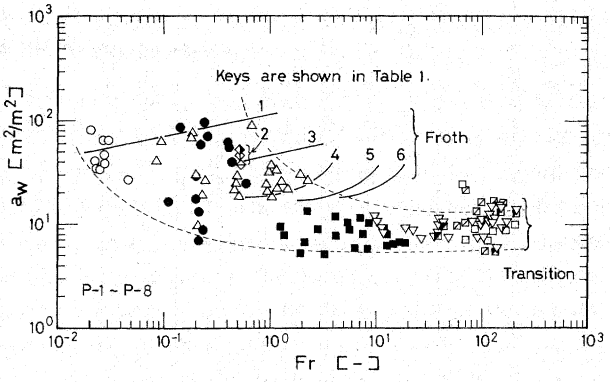


Fig. 4. Gas-liquid interfacial area on the basis of bubbling area

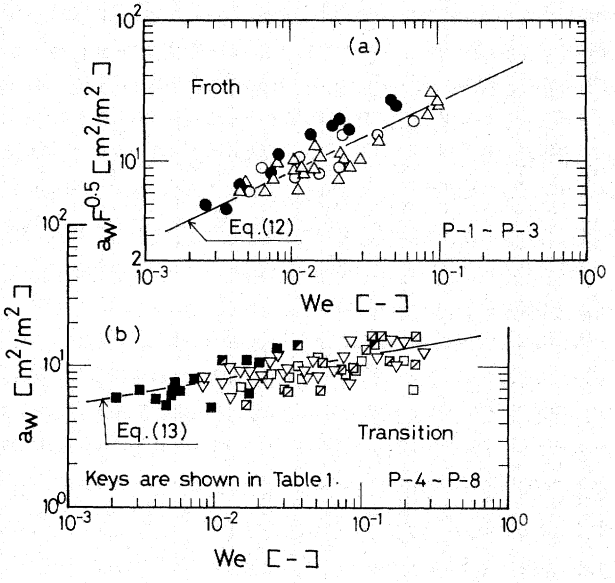


Fig. 5. Correlation of interfacial area

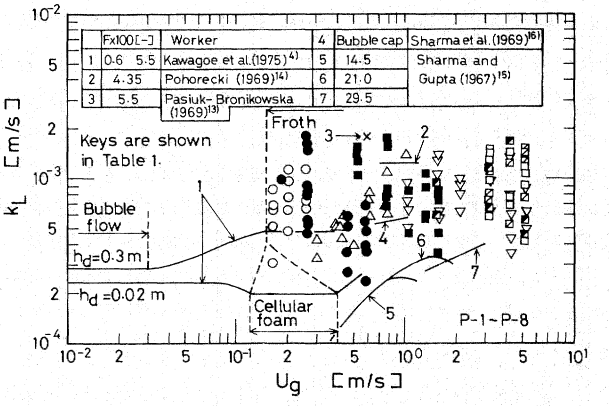


Fig. 6. Mass transfer coefficient

Kawagoe *et al.*[4] Due to the large free area of sieve plates used in the present study, leading to a different flow regime, namely the transition regime, it is hard to compare the present results directly with those of Kawagoe *et al.* The results for P-1–P-3 showing the froth regime, however, are similar to those of Kawagoe

et al. The scatter of experimental values is presumable explained by the liquid holdup, as the increase in liquid velocity is related to the variation of liquid holdup. Therefore, it seems that the effect of liquid velocity probably reduces to that of liquid holdup. In fact, Asano *et al.*[2] noticed the effect of liquid holdup on the liquid-phase mass transfer coefficient under gas-liquid cross-current flow conditions. According to the theoretical treatment of a single bubble, the Sherwood number involving mean bubble diameter for a bubble swarm in a bubble column and a plate column should be correlated with a dimensionless group such as the Schmidt number and the Reynolds number. In the present study, according to Kawagoe *et al.*[4], the Galilei number, which represents circulation of viscous flow, is used instead of the Reynolds number involving relative velocity—the measurement of which is virtually impossible. It is, however, also impossible to take mean bubble diameter as characteristic length for the above-mentioned dimensionless groups. We tried, therefore, to correlate the Sherwood number involving liquid holdup due to the significant dependence on gas-liquid interfacial area, probably leading to bubble diameter as follows:

$$Sh = f(Sc, Ga) \tag{14}$$

Figure 7 shows the correlation of the mass transfer coefficient. The mass transfer coefficient. for both the froth regime and the transition regime are expressed by the following expressions, taking account of the result of Kawagoe *et al.*[4] which showed that Sh is proportional to $Sc^{1/2}$

$$Sh = 3.37 Sc^{1/2} Ga^{1/4} \quad \text{froth regime} \tag{15}$$

$$Sh = 0.07 Sc^{1/2} Ga^{1/2} \quad \text{transition regime (partially developed spray/mixed froth)} \tag{16}$$

2.4 Liquid-phase volumetric mass transfer coefficient

The correlations for gas-liquid interfacial area and liquid-phase mass transfer coefficient are obtained for plate columns with plates having large free areas without downcomer capable of being operated at greater gas velocities than those for the usual plate columns. Usually, the volumetric mass transfer coefficients frequently used for the design and the operation of these devices are obtained as the product of interfacial area and mass transfer coefficient. **Table 3** summarizes the results obtained in the present study. The parity plot for liquid-phase volumetric mass transfer coefficient using Eqs. (17) and (18) is indicated by **Fig. 8** and shows good agreement with the measurements.

Concluding Remarks

Gas-liquid interfacial areas and liquid-phase mass transfer coefficients were measured for plates without a downcomer having large free areas and operated at high gas velocities during mass transfer experiments in cobalt-catalyzed oxidation of aqueous sodium sulfite solutions with air. The following results were obtained:

1) The two-phase dispersion on a sieve plate shows that the froth regime and the transition regime is dependent on gas velocities and the complete spray regime does not appear in plate columns without downcomer.
2) The gas-liquid interfacial area is correlated well on a unit bubbling area basis, that is, as a_w as a function of the Weber number proposed by Zuiderweg.[23]

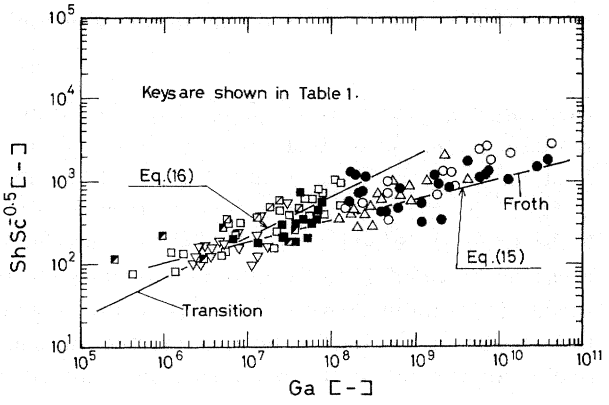


Fig. 7. Correlation of mass transfer coefficient

Table 3. Correlations of a_L, k_L and $k_L a_L$

	Froth regime		Transition regime	
a_L	$a_L h_L = 80 We^{0.5}/F^{0.5}$	(12)	$a_L h_L = 19.1 We^{0.2}$	(13)
k_L	$Sh = 3.37 Sc^{1/2} Ga^{1/4}$	(15)	$Sh = 0.07 Sc^{1/2} Ga^{1/2}$	(16)
$k_L a_L$	$\frac{K_L a_L h_L^2}{D_A} = 270 Sc^{1/2} Ga^{1/4} \times We^{1/2} F^{-1/2}$	(17)	$\frac{k_L a_L h_L^2}{D_A} = 1.34 Sc^{1/2} Ga^{1/2} \times We^{0.2}$	(18)

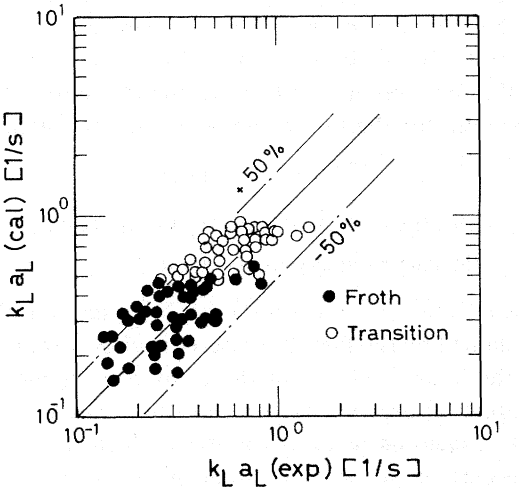


Fig. 8. Parity plot for volumetric mass transfer coefficient

3) Empirical equations of liquid-phase mass transfer coefficient in each operating regime, froth and transition, are obtained on the basis of the Sherwood number, the Schmidt number and the Galilei number involving liquid holdup corresponding to gas and liquid velocities.

Nomenclature

a_L	=	effective interfacial area per unit volume of liquid	[m^2/m^3]
a_F	=	effective interfacial area per unit volume of froth	[m^2/m^3]
a_w	=	effective interfacial area per unit bubbling area	[m^2/m^3]
C_{Ai}	=	concentration of solute gas at the interface	[mol/m^3]
C_{AL}	=	concentration of solute gas in the liquid bulk	[mol/m^3]
C_{B1}	=	concentration of Na_2SO_3 fed into the column	[mol/m^3]
C_{B2}	=	concentration of Na_2SO_3 in liquid on the plate	[mol/m^3]
C_{BL}	=	concentration of Na_2SO_3 in the liquid bulk	[mol/m^3]
C_{CoSO_4}	=	concentration of $CoSO_4$	[mol/m^3]
D_A	=	diffusivity of solute gas in the solution	[m^2/s]
D_B	=	diffusivity of Na_2SO_3 in the solution	[m^2/s]
d	=	hole diameter	[m]
d_B	=	mean bubble diameter	[m]
F	=	free area	[—]
Fr	=	Froude number $= U_g^2/(gh_L)$	[—]
Ga	=	Galilei number $= gh_L^3/v_L^2$	[—]
H	=	Henry's constant	[—]
h_d	=	downcomer height	[m]
h_L	=	liquid holdup	[m]
k_L	=	liquid-phase mass transfer coefficient	[m/s]
k_La_L	=	liquid-phase volumetric mass transfer coefficient	[s^{-1}]
k_2	=	rate constant of second-order reaction	[$m^3/mol \cdot s$]
n	=	number of plates	[—]
p	=	*pitch*	[m]
P_{O_2}	=	partial pressure of oxygen	[Pa]
R	=	gas constant	[$Pa \cdot m^3/mol \cdot K$]
R_A	=	mass transfer rate	[$mol/m^3 \cdot s$]
Sc	=	Schmidt number $= v_L/D_A$	[—]
Sh	=	Scherwood number $= k_Lh_L/D_A$	[—]
T	=	absolute temperature	[K]
U_g, U_L	=	superficial velocity of gas and liquid	[m/s]
We	=	Weber number $= h_L\rho_g^{0.5}U_g\rho_L^{0.5}U_L/\sigma$	[—]
x	=	distance from gas-liquid interface	[m]
β_∞	=	enhancement factor	[—]
γ	=	Hatta number	[—]
μ_g, μ_L	=	viscosity of gas and liquid	[$Pa \cdot s$]
v_L	=	kinematic viscosity of liquid	[m^2/s]
ρ_L, ρ_g	=	density of gas and liquid	[kg/m^3]
σ	=	surface tension	[N/m]

Literature Cited

1) Asano, K. and S. Fujita: *Kagaku Kōgaku*, **28**, 926 (1964).
2) Asano, K. and S. Fujita: *Kagaku Kōgaku*, **30**, 403 (1966)
3) Danckwerts, P. V.: "Gas-Liquid Reactions," McGraw-Hill (1970).
4) Kawagoe, M., K. Nakao and T. Otake: *J. Chem. Eng. Japan*, **8**, 254 (1975).
5) Kimura, M., K. Nakao and Y. Yasuda: *Kagaku Kogaku Ronbunshu*, **8**, 358 (1982).
6) Linek, V. and V. Vacek: *Chem. Eng. Sci.*, **36**, 1747 (1981).
7) Miller, D. N.: *AIChE J*, **39**, 312 (1983).
8) Miyahara, T., H. Terakado and T. Takahashi: *J. Chem. Eng. Japan*, **16**, 454 (1983).
9) Miyahara, T. and T. Takahashi: *J. Chem. Eng. Japan*, **17**, 218 (1984).
10) Miyahara, T. and T. Takahashi: *J. Chem. Eng. Japan*, **17**, 211 (1984).
11) Miyahara, T., Y. Tanaka, Y. Iwamoto and T. Takahashi: *Int. J. Eng. Fluid Mech.*, **2**, 235 (1989).
12) Nagy, E., O. Borlai, E. Laurent and J.-C. Charpentier: *Int. Chem. Eng.*, **15**, 637 (1975).
13) Pasiuk-Bronikowska, W.: *Chem. Eng. Sci.*, **24**, 1139 (1969).
14) Pohorecki, R.: *Int. Chem. Eng.*, **15**, 647 (1975).
15) Sherma, M. M. and R. K. Gupta: *Trans. Instn. Chem. Engrs.*, **45**, T169 (1967).
16) Sharma, M. M., and R. A. Mashelkar and V. D. Mehta: *Brit. Chem. Eng.*, **14**, 70 (1969).
17) Smith, R. K. and G. Wills: *Ind. Eng. Chem. Proc. Des. Develop.*, **5**, 39 (1966).
18) Takahashi, T., R. Matsuno and T. Miyahara: *J. Chem. Eng. Japan*, **6**, 38 (1973).
19) Takahashi, T., T. Miyahara and K. Shimizu: *J. Chem. Eng. Japan*, **7**, 75 (1974).
20) Takahashi, T., T. Miyahara, T. Tano and Y. Akagi: *J. Chem. Eng. Japan*, **19**, 339 (1986).
21) Thomas, W. J. and M. A. Haq: *Ind. Eng. Chem., Proc. Des. Develop.*, **15**, 509 (1976).
22) Thomas, W. J. and O. Ogboja: *Ind. Eng. Chem., Proc. Des. Develop.*, **21**. 217 (1982).
23) Zuiderweg, F. J.: *Chem. Eng. Sci.*, **37**, 1441 (1982).

(Presented at the Autumn Meeting of the Society of Chemical Engineers, Japan, at Fukuoka, October 1988).